© 2023. Published by The Company of Biologists Ltd | Journal of Experimental Biology (2023) 226, jeb244295. doi:10.1242/jeb.244295

RESEARCH ARTICLE

Influence of surface free energy of the substrate and flooded water on the attachment performance of stick insects (Phasmatodea) with different adhesive surface microstructures

Julian Thomas*, Stanislav N. Gorb and Thies H. Büscher

ABSTRACT

Stick and leaf insects (Phasmatodea) are exclusively herbivores. As they settle in a broad range of habitats, they need to attach to and walk on a wide variety of plant substrates, which can vary in their surface free energy (SFE). The adhesive microstructures (AMs) on the euplantulae of phasmids are assumed to be adapted to such substrate properties. Moreover, the natural substrates can often be covered with water as a result of high relative humidity or rain. Although considerable experimental research has been carried out on different aspects of stick insect attachment, the adaptations to cope with the influence of flooded water on attachment performance remain unclear. To elucidate the role of AMs in this context, we here measured attachment forces in three species of stick insects with different AMs. The results show that attachment forces of the three species studied were influenced by the SFE and the presence of water: they all showed higher pull-off (vertical) and traction (horizontal) forces on dry surfaces, compared with when the surfaces were covered with a water film. However, the extent to which the surface properties influenced attachment differed depending on the species and its AMs. All three species showed approximately the same attachment performance on dry surfaces with different surface free energy but maintained attachment underwater to different extents.

KEY WORDS: Biomechanics, Functional morphology, Friction, Adhesion, Tarsus morphology, Locomotion

INTRODUCTION

The ability of organisms to attach to and detach from surfaces is often essential for their survival. Attachment systems used for terrestrial locomotion evolved convergently in different animal lineages; for example, in squamates, amphibians and arthropods (Gorb, 2001; Scherge and Gorb, 2001; Persson, 2003; Federle et al., 2000; Federle, 2006; Federle et al., 2006; Büscher et al., 2019; Büscher and Gorb, 2021). Organisms of great interest for this study are Phasmatodea, colloquially known as stick insects. They are terrestrial herbivorous insects that inhabit a high diversity of habitats worldwide (Bedford, 1978; Brock et al., 2022). These insects are strongly adapted to plants, as visible in their cryptic mimicry, i.e. their leaf- and twig-like appearance, and presumably co-evolved with them (Wang et al., 2014; Bank et al., 2021a,b). This co-evolution shaped the attachment systems of phasmids, enabling them to attach to a wide variety of plant surfaces (Büscher et al., 2018a,b, 2019; Büscher and Gorb, 2019).

Their tarsal attachment system consists of three main units. The first unit is the euplantulae, which, depending on the species, are situated on the first to fourth or first to fifth tarsomeres (Beutel and Gorb, 2006). They are covered with a diversity of different species-specific adhesive microstructures (AMs) (Büscher et al., 2018a,b, 2019). It has been previously assumed that these microstructures evolved as adaptations to the substrates the animals are exposed to (Büscher and Gorb, 2017; Büscher et al., 2018a; Cumming et al., 2021). The euplantulae as such enable a trade-off between generating stationary attachment and propulsion for locomotion (Gorb et al., 2000; Jiao et al., 2000; Federle, 2006; Bußhardt et al., 2012; Büscher et al., 2018a).

The second unit involved in attachment is the two pretarsal claws, used for interlocking with rough surface asperities, and an arolium in between them as the third unit. The latter is rather soft and used to increase the contact area to the surface and by this to enhance the attachment forces (Clemente and Federle, 2008). Phasmids rely on ‘wet adhesion’, meaning that they produce an adhesive fluid that influences attachment (Dirks et al., 2010). *Hermarchus leytensis* has been shown to possess pores on the pads (Gottardo and Vallotto, 2014), through which the fluid is secreted. It then interacts with the surface and increases the contact area, resulting in stronger adhesion.

In general, the forces involved in insect adhesion can be divided into two groups: those that arise during dry interactions – the van-der-Waals forces, chemical bonds and friction; and those caused by the adhesive fluid produced by insects – the capillary and viscous forces (Stefan, 1875; Johnson, 1998; Dirks, 2014; Ditsche and Summers, 2014; Popov, 2016; Büscher and Gorb, 2021; Meng et al., 2021). Chemical analysis of the adhesive fluid of insects indicated an emulsion composed of rather different constituents, such as unipolar carbohydrates, fatty acids, polar proteins and peptides, resulting in stronger adhesion to substrates with different surface energies and polarities (Attygall et al., 2000; Vötsch et al., 2002; Dirks et al., 2010; Dirks and Federle, 2011; Betz et al., 2018). Studies investigating the components of adhesive secretions have shown that they can differ greatly between groups of insects (Attygall et al., 2000; Vötsch et al., 2002; Dirks et al., 2010; Dirks and Federle, 2011; Betz et al., 2018). These differences in composition can therefore influence the attachment of the insects.

Attachment of phasmids is constrained by many factors, for example roughness, mechanical and chemical properties and inclination of the surface, of which some have been investigated already. Studies regarding the effect of surface roughness on phasmid attachment have shown that the AMs determines the attachment performance on different rough surfaces

Functional Morphology and Biomechanics, Institute of Zoology, Kiel University, Am Botanischen Garten 9, 24118 Kiel, Germany.

*Author for correspondence (jthomas@zoologie.uni-kiel.de)

J.T., 0000-0002-7923-7013; S.N.G., 0000-0001-9712-7953

Received 18 March 2022; Accepted 28 December 2022

Journal of Experimental Biology (2023) 226, jeb244295. doi:10.1242/jeb.244295

(Bußhardt et al., 2012; Büscher and Gorb, 2019). The animals examined in this study possess smooth (*Medauroidea extradentata*), nubby (*Sungaya inexpectata*) or hexagonal (*Epidares nolimetangere*) AMs. Species with smooth AMs on their euplantulae generate stronger adhesion on smooth substrates compared with species with nubby AMs, which perform better on micro-rough surfaces (Bußhardt et al., 2012; Büscher and Gorb, 2019). The function of hexagonal AMs has not been previously studied in phasmids, but has in other animals and artificial systems (Federle et al., 2006; Varenberg and Gorb, 2009; Drotlef et al., 2013).

Another factor of substrates that influences adhesion is the surface chemistry, measured by the surface free energy (SFE). Substrates with a high SFE are hydrophilic, have a low contact angle ($\theta<90$ deg) with water and therefore show a good wettability of the surface. A low SFE indicates that the substrate is hydrophobic, has a high contact angle ($\theta>90$ deg) with water and shows poor wettability of the surface. Plants are particularly important for the herbivorous Phasmatodea as substrates for attachment. Along with other purposes, low SFE of plant surfaces is one strategy to avoid attachment of herbivorous insects (Gorb and Gorb, 2009). Plant surfaces often have a low SFE, whereby it has an influence on attachment (Voigt and Gorb, 2009; Gorb and Gorb, 2017). Some insectivorous plants exploit the interaction between high SFE and a humidity-induced water film on the attachment. This has been shown by Labonte et al. (2021) for the surface of the pitcher plant *Nepenthes fusca*, which has a high SFE, enabling it to effectively hold a water film to strongly reduce the attachment forces of insects. Insect anti-adhesive effect arises from the combination of surface chemistry and texture, but it is primarily driven by the substrate roughness, and less by the surface chemistry (England et al., 2016).

In the present study, we investigated the influence of three different substrates with different SFE (glass, silanized glass and Teflon) on the pull-off and traction forces of three stick insect species with different AMs. Furthermore, we analyzed the pull-off and traction forces on all three substrates with and without water film to investigate the effect of water presence and SFE regarding the attachment performance. Specifically, we asked the following questions. (i) How does SFE of the substrate influence the pull-off and traction forces of the three stick insect species? (ii) How does the water film influence the pull-off and traction forces? (iii) How does the combination of specific SFE and the presence of the water film affect the attachment performance of the three species? (iv) How do pull-off and traction forces differ between the species with nubby, hexagonal and smooth AMs on their euplantulae?

MATERIALS AND METHODS

Animals

The species in this study were selected according to the AMs on their euplantulae (see Büscher et al., 2019). *Sungaya inexpectata* Zompro 1996 (Fig. 1A) possesses nubby AMs. The euplantulae of *Epidares nolimetangere* (de Haan 1842) (Fig. 1B) exhibit hexagonal patterned (plateaus) AMs. *Medauroidea extradentata* Brunner von Wattenwyl 1907 (Fig. 1C) has smooth AMs (Fig. 2). All individuals used were obtained from the laboratory cultures of the Department of Functional Morphology and Biomechanics (Kiel University, Germany). The insects were fed with blackberry leaves *ad libitum* and kept on a regular day and night cycle. Only adult individuals with all six legs intact were selected. The adhesive system of all individuals was tested on a glass plate prior to the experiments: if they were unable to show any pull-off forces, they were not selected for further experiments.

Force measurements

All specimens were attached to a force transducer (*S. inexpectata* and *M. extradentata*: 100 g capacity, FORT100, World Precision Instruments Inc., Sarasota, FL, USA; *E. nolimetangere*: 25 g capacity, FORT25, World Precision Instruments Inc.) by gluing a hair onto the metanotum of the stick insects with beeswax. The force transducers were connected to a BIOPAC Model MP100 and a BIOPAC TCI-102 System (BIOPAC Systems, Inc., Goleta, CA, USA). Force–time curves were recorded with AcqKnowledge 3.7.0 software (BIOPAC Systems Inc.).

The highest peak of the obtained graph was considered as the maximum attachment force for further processing (Fig. 3C,D). For the recording of the traction forces, the force transducer was aligned horizontally at the same height as the insect. The substrate was then pulled back from the animal (Fig. 3B). For measuring the pull-off force, the force transducer was positioned above the insect and the substrate was pulled away from the animal in the direction orthogonal to the sensor (Fig. 3A). In both experiments, the surface was moved manually at a steady speed with a winch; the speed for the pull-off force measurements was around 0.5–1.0 cm s^{-1} and that for the traction force measurements was around 1.0–3.0 mm s^{-1}. The irregular increases of the traction and pull-off forces prior to the maximum forces (Fig. 3C,D) represent the normal stick and slip response of the stick insects (Büscher et al., 2020).

For each species, pull-off and traction force measurements were conducted. A total of six different substrates were used: three surfaces with different SFE (see below), each of them in the dry condition and with a thin water film. The measurements were performed with the same individuals per species (*S. inexpectata* $N=13$, *E. nolimetangere* $N=24$, *M. extradentata* $N=11$), which were measured 3 times in a row. The mean value of the three measurements was calculated to reduce the intra-individual variance. The sequence of individuals was randomized for every substrate. In order to hold a stable thin water film on the surface for the wet measurements, an additional border of dental wax was

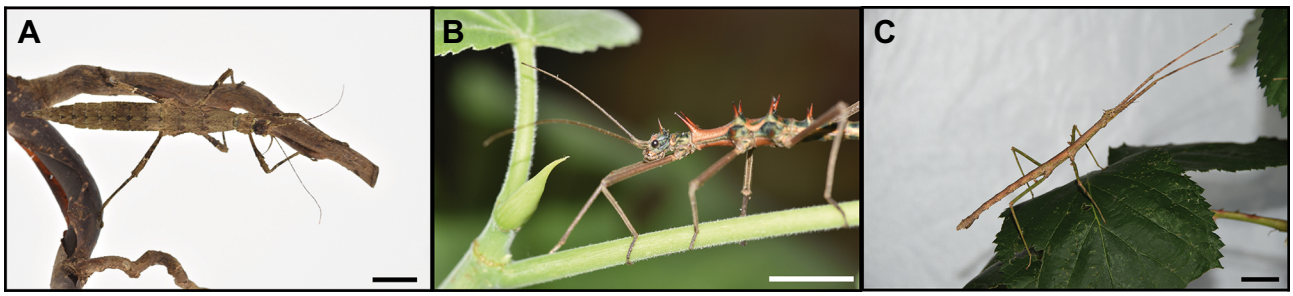

Fig. 1. Species used in this study. Adult female *Sungaya inexpectata* (A), adult male *Epidares nolimetangere* (B) and adult female *Medauroidea extradentata* (C). Scale bars: 20 mm.

Journal of Experimental Biology (2023) 226, jeb244295. doi:10.1242/jeb.244295

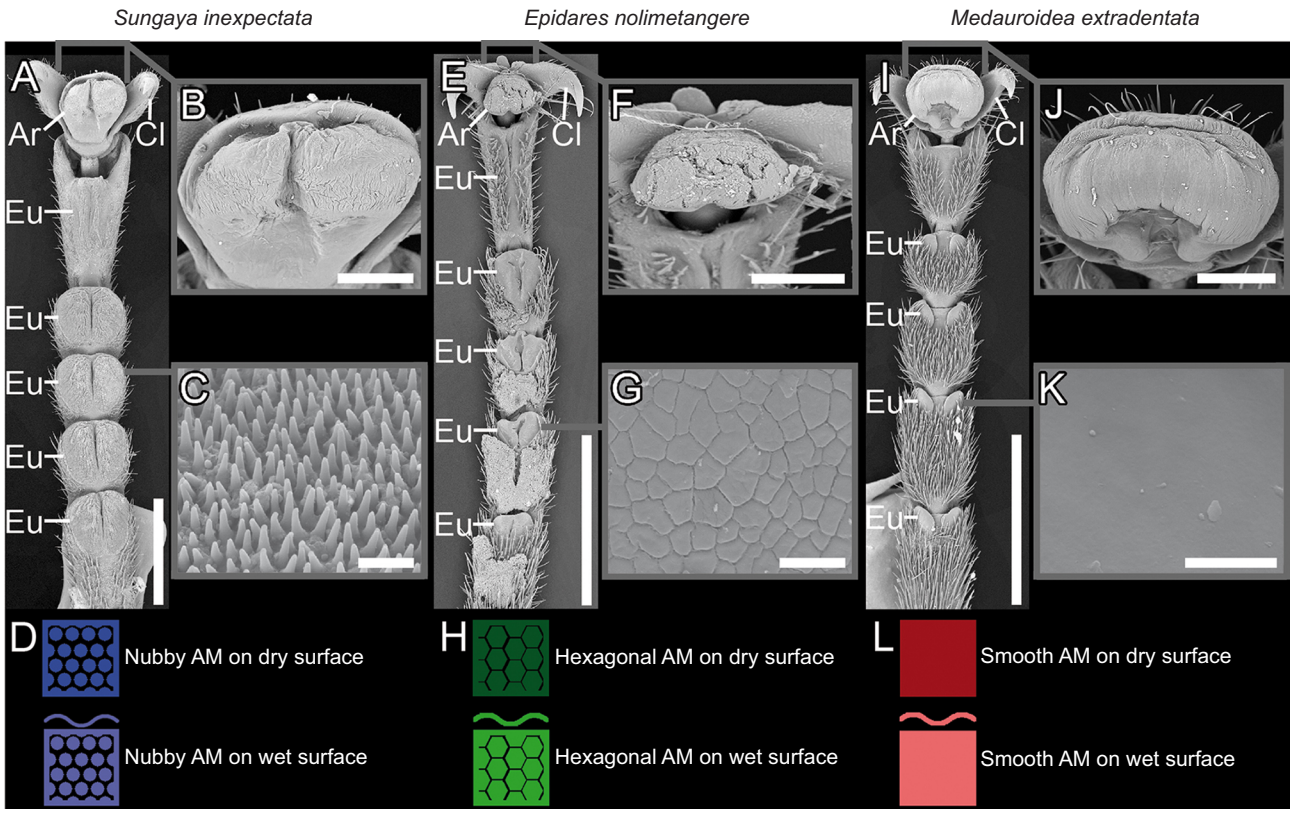

Fig. 2. Tarsal structures of the species used in this study. (A,E,I) Tarsus overview. Scale bars: 1 mm. (B,F,J) Arolium. Scale bars: 300 µm. (C,G,K) Attachment microstructure (AM) of euplantulae. Scale bars: 10 µm. (D,H,L) Pictogram symbols for the wet and dry substrates. Ar, arolium; Cl, claw; Eu, euplantulae.

added (Fig. 3A,B). This edge produced a water film (approximately 2–3 mm thick) that covered the entire surface. During the measurements on the surfaces with a thin water film, it was always ensured that the entire adhesive organ of the phasmid was covered by water. Ditsche and Summers (2014) describe such conditions as immersed conditions.

The sex of the specimens was kept the same per species, to ensure the same AMs and body proportions within the groups. For

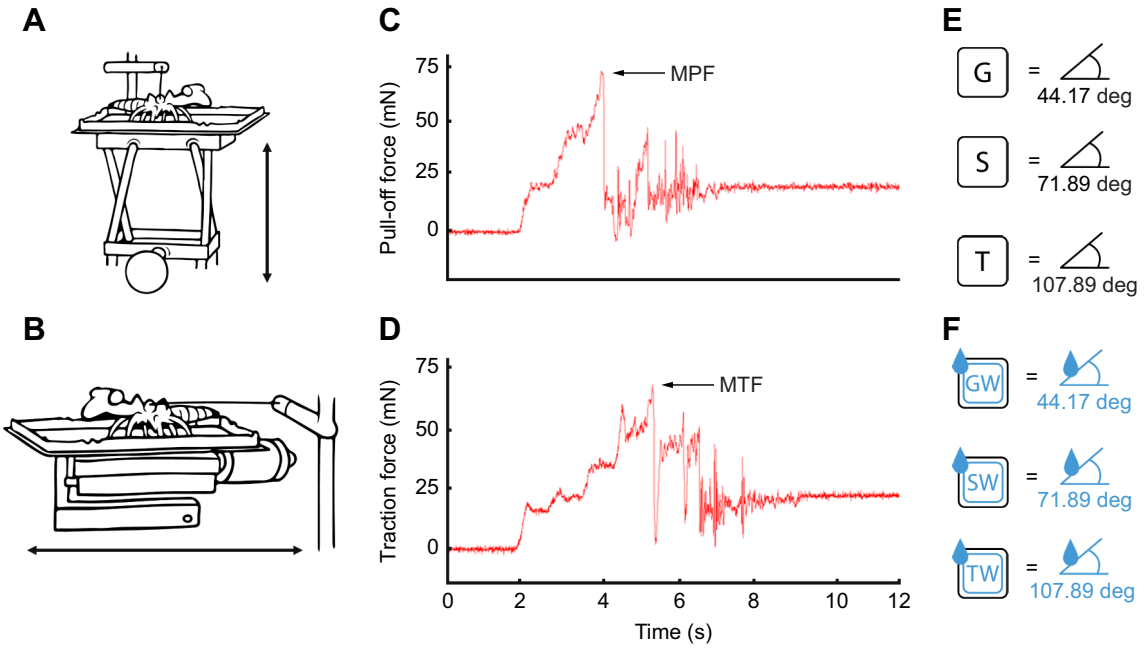

Fig. 3. Experimental setup. (A,B) Schematic setup of (A) pull-off force and (B) traction force measurements. Arrow indicates the direction of pulling. (C,D) Example curves for (C) pull-off force and (D) traction force measurements. MPF, maximum pull-off force; MTF, maximum traction force. (E,F) Pictograms indicating the different dry (E) and wet (F) surfaces (G, glass; S, silanized glass; T, Teflon; W, wet) with corresponding contact angles.

S. inexpectata (mean±s.d. body mass 2.79±0.88 g) and *M. extradentata* (body mass 1.10±0.04 g), females were used, whereas for *E. nolimetangere* (body mass 0.78±0.08 g), males were used. Ambient humidity in the laboratory was around 45–58% at a temperature of 21–23°C.

All individuals were tested in all treatments. The individuals did not show any signs of exhaustion during the series of measurements. Each individual contributed equally to the experiments.

Substrate preparation

A glass surface (G) was used as the hydrophilic surface with high SFE and another glass surface was silanized (S), as described by Voigt and Gorb (2009), to decrease the SFE of the surface. The third surface used was Teflon (T) as a low SFE surface. The physico-chemical properties of the surfaces were characterized by measuring the contact angle of water on the substrate (aqua Millipore, droplet size 1 µl, sessile drop method; n=10 per substrate) using the contact angle measurement instrument OCAH 200 (Dataphysics Instruments GmbH, Filderstadt, Germany). The contact angle was 44.17±7.74 deg for glass surface, 71.69±8.02 deg for the silanized glass surface and 107.89±1.22 deg for Teflon (Fig. 3E,F). The surfaces with a continuous water film are referred to below as glass with water film (GW), silanized glass with water film (SW) and Teflon with water film (TW).

The arithmetic average roughness (R_a) of Teflon was measured with a 3D measurement microscope (Keyence VR 3100, KEYENCE, Neu-Isenburg, Germany). The roughness profile of 10 lines with an approximate length of 1 mm in the horizontal and vertical direction was evaluated.

Statistical analysis

The statistical analyses were performed using SigmaPlot 12.0 (Systat Software Inc., San José, CA, USA). The data were tested for normal distribution (Shapiro–Wilk test) and homoscedasticity (Levene's test) before subsequent tests. Pull-off and traction forces on the different surfaces with and without water film for each species were compared using Kruskal–Wallis one-way analyses of variance (ANOVA) on ranks and Tukey's *post hoc* test, as the data were neither normally distributed nor showed homoscedasticity.

Differences between the three species were analyzed with Kruskal–Wallis one-way ANOVA on ranks and Dunn's *post hoc* test. For all statistical comparisons, the significance level (alpha) was set to 0.05.

To determine the influence of the wet surfaces on the attachment, the attachment on the dry surfaces was assumed to be the maximum attachment (100%). The percentage loss of attachment was calculated by subtracting the remaining attachment (%) on the wet surfaces from 100%. This allowed us to calculate the percentage reduction between the attachment forces on the dry and the wet substrates.

Adhesive performance representations

The pull-off and traction forces were compared between the species with two approaches. To account for the different weights of the species, the safety factor (SF) was calculated:

$$\mathrm{SF} = \frac{F_a}{F_w}, \quad (1)$$

where F_a is the attachment force and F_w is the weight force.

The weight force (F_w) was calculated from the mass of the species (m) and the gravitational constant ($\boldsymbol{g}$):

$$F_w = m\boldsymbol{g}. \quad (2)$$

To account for the different areas of the attachment pads across the species, adhesive (for pull-off) and shear (for traction) strength were used. For this purpose, five tarsi were cut from *S. inexpectata* and *M. extradentata* adult females and five tarsi were cut from *E. nolimetangere* adult males. The ventral side of the tarsi was scanned with the Keyence VR 3100 (KEYENCE) and the projected pad areas of the attachment pads (euplantulae and arolium) were measured. To calculate the adhesive and shear strength for each species, the pull-off or traction forces were divided by the average total adhesive surface area, which was obtained by adding up the surface area of the arolium and euplantulae (multiplied by 6, as the animals have six legs):

$$\text{Adhesive/Shear strength} = \frac{F_{\text{Pull-off / Traction}}}{\text{Average total adhesive surface area}}. \quad (3)$$

Scanning electron microscopy

Tarsi of *S. inexpectata* and *M. extradentata* were cut from adult females and tarsi of *E. nolimetangere* from adult males. They were fixed in 1 ml Bouin's fixative for 24 h on a shaker. Afterwards, the samples were dried in an ascending ethanol series, critical point dried (Leica EM CPD300, Leica, Wetzlar, Germany) and sputter-coated with a 10 nm layer of gold–palladium (Leica Bal-TEC SCD500). The samples were mounted on a rotatable specimen holder (Pohl, 2010) and the images were obtained using a scanning electron microscope (TM3000, Hitachi High-technologies Corp., Tokyo, Japan) at 15 kV acceleration voltage. Focus stacks of the part of interest were recorded. They were stitched, merged and processed using the software Photoshop CS5 (Adobe Systems Inc., San Jose, CA, USA).

RESULTS

Tarsal morphology

All species studied possess a tarsus with five tarsomeres as well as a pretarsus with two claws and an arolium in between. The main difference between the species is in the AMs: *S. inexpectata* has euplantulae on tarsomeres 1–5, each with nubby AMs (Fig. 2A–D); *E. nolimetangere* possesses euplantulae with hexagonal AMs on tarsomeres 1–5 (Fig. 2E–H); and *M. extradentata* has smooth euplantulae which are located on tarsomeres 1–4 (Fig. 2I–L).

Attachment performance

Sungaya inexpectata

The measured impact of SFE and water on the pull-off forces of *S. inexpectata* with nubby AMs revealed significantly larger values on the dry surfaces (mean±s.d. G 104.15±48.14 mN, S 113.04±59.74 mN and T 78.18±36.16 mN) than on the surfaces with a water film (GW 9.36±15.23 mN, SW 37.39±22 mN and TW 16.76±18.28 mN) (Kruskal–Wallis one-way ANOVA on ranks, H=55.31, d.f.=5, $P \leq 0.001$, N=13). For the surfaces with a water film, only the pull-off forces between SW and GW were significantly different (Kruskal–Wallis one-way ANOVA on ranks, H=10.496, d.f.=2, P=0.005, N=13) (Fig. 4A).

The same impact was found for both SFE and water on the traction force (G 228.37±159.97 mN, S 148.67±102.11 mN, T 146.17±71.55 mN, GW 32.46±17.47 mN, SW 59.27±24.75 mN and TW 45.41±27.66 mN) (Kruskal–Wallis one-way ANOVA on

Journal of Experimental Biology (2023) 226, jeb244295. doi:10.1242/jeb.244295

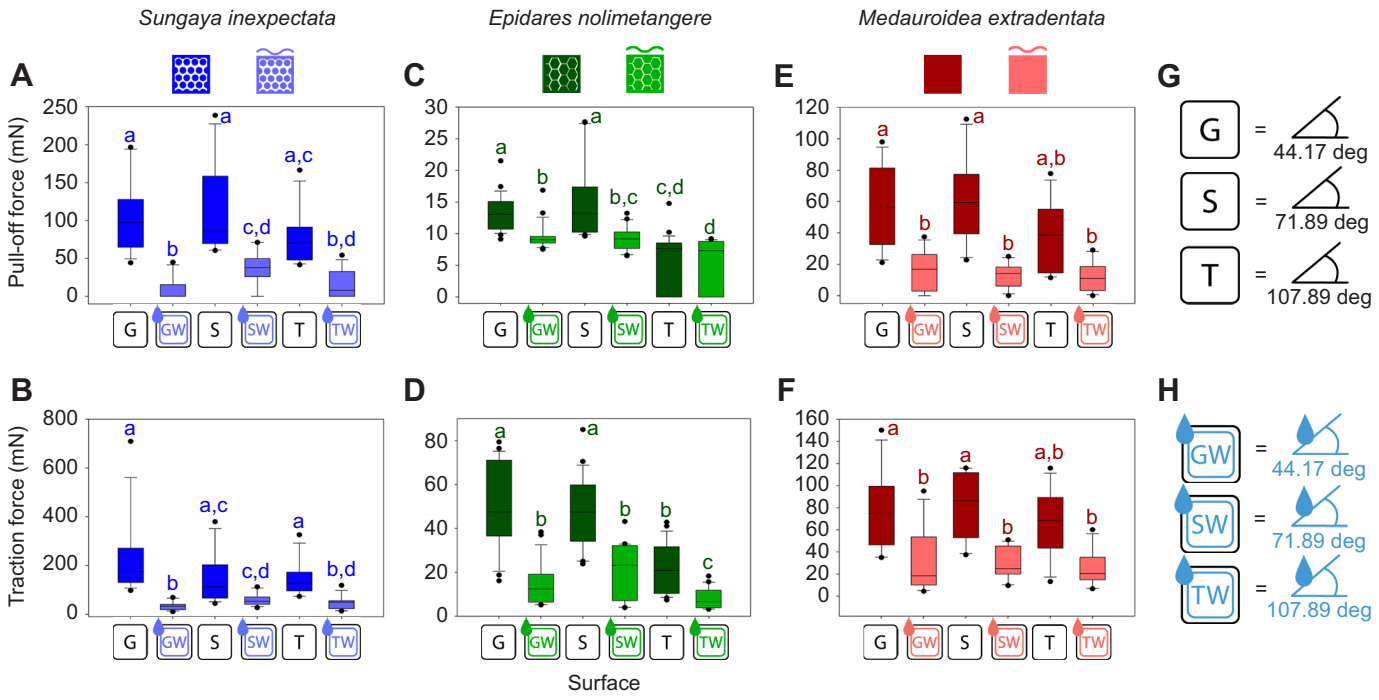

Fig. 4. Pull-off and traction forces of the three species studied on different surfaces. (A,C,E) Pull-off force and (B,D,F) traction force of *S. inexpectata* (blue; *n*=13), *E. nolimetangere* (green; *n*=24) and *M. extradentata* (red; *n*=11). The values correspond to the means of the triplet measurements per individual. Groups with different lowercase letters are statistically different (Kruskal–Wallis one-way ANOVA on ranks with Tukey's *post hoc* test, $P<0.05$). Boxes indicate the 25th and 75th percentiles, whiskers are the 10th and 90th percentiles and the line within the boxes shows the median. Dark colors of the boxes indicate dry surfaces; light colors of the boxes indicate surfaces with a water film. (G,H) Pictograms indicating the different dry (G) and wet (H) surfaces (G, glass; S, silanized glass; T, Teflon; W, wet) with corresponding contact angles.

ranks, H=8.384, d.f.=2, P=0.015; Kruskal–Wallis one-way ANOVA on ranks, H=53.297, d.f.=5, $P\leq0.001$, N=13) (Fig. 4B).

Epidares nolimetangere

For *E. nolimetangere* with hexagonal AMs, the impact of the SFE and water resulted in significantly higher pull-off forces on the two dry surfaces G and S than on all other surfaces (G 13.18±2.85 mN, S 14.80±5.64 mN, T 5.14±4.65 mN, GW 9.62±2.04 mN, SW 9.23±1.86 mN and TW 5.10±4.09 mN) (Kruskal–Wallis one-way ANOVA on ranks, H=90.685, d.f.=5, $P\leq0.001$, N=24) (Fig. 4C). The value on GW was significantly higher than those on T and TW. Additionally, the value on SW was significantly higher than that on TW (Kruskal–Wallis one-way ANOVA on ranks, H=90.685, d.f.=5, $P\leq0.001$, N=24).

The impact of SFE and water on the traction force also revealed significantly higher values on the dry surfaces G and S than on all other surfaces (G 50.68±19.35 mN, S 47.30±16.11 mN, T 20.94±10.35 mN, GW 12.40±6.43 mN, SW 23.25±7.12 mN and TW 6.63±3.87 mN) (Kruskal–Wallis one-way ANOVA on ranks, H=87.523, d.f.=5, $P\leq0.001$, N=24, q=5.65) The traction forces on the surfaces GW, SW and T were significantly higher compared with that on TW (Kruskal–Wallis one-way ANOVA on ranks, H=87.523, d.f.=5, $P\leq0.001$, N=24; Kruskal–Wallis one-way ANOVA on ranks, H=18.179, d.f.=2, $P\leq0.001$, N=24) (Fig. 4D).

Medauroidea extradentata

The impact of SFE and water on the pull-off force of *M. extradentata* (smooth AMs) revealed significantly higher values on the two dry surfaces G and S when compared with the wet surfaces (G 56.75±26.15 mN, S 61.11±12.26 mN, T 37.75±22.42 mN, GW 16.12±12.26 mN, SW 12.85±7.50 mN and TW 12.55±9.04 mN) (Kruskal–Wallis one-way ANOVA on ranks, H=38.597, d.f.=5, $P\leq0.001$, N=11). No significant differences could be observed between the pull-off forces on T and the three wet surfaces (Fig. 4E).

The same results were obtained when comparing the traction forces (G 76.53±35.28 mN, S 78.60±29.47 mN, T 64.27±30.06 mN, GW 30.08±28.28 mN, SW 30.18±14.64 mN and TW 25.65 1±6.06 mN) (Kruskal–Wallis one-way ANOVA on ranks, H=30.127, d.f.=5, $P\leq0.001$, N=11) (Fig. 4F).

Comparison of the pull-off force safety factors between the three species

The pull-off force safety factors of the species *M. extradentata* and *S. inexpectata* on the dry substrates G and S were significantly higher than the values for *E. nolimetangere* (*S. inexpectata*: G 3.92±1.74, S 4.26±1.90, T 3.06±1.75; *M. extradentata*: G 5.06±1.78, S 5.70 ±1.49, T 3.47±1.58; *E. nolimetangere*: G 1.69±0.36, S 1.89±0.74, T 0.70±0.64) (Fig. 5A). The values of *S. inexpectata* and *M. extradentata* on T and of *E. nolimetangere* on S were significantly different to the value of *E. nolimetangere* on T (Kruskal–Wallis one-way ANOVA on ranks, H=103.599, d.f.=8, $P\leq0.001$; *S. inexpectata* N=13, *E. nolimetangere* N=24, *M. extradentata* N=11).

On the wet substrates, the pull-off force safety factors only showed significant differences between the values of *S. inexpectata* on SW and those of *S. inexpectata* on GW and *E. nolimetangere* on TW (*S. inexpectata* GW 0.48±0.74, SW 1.69±1.14, TW 0.60±0.67; *M. extradentata* GW 1.40±0.95, SW 1.56±1.36, TW 1.18±0.84; and *E. nolimetangere* GW 1.30±0.32, SW 1.18±0.15, TW 0.68±0.54) (Kruskal–Wallis one-way ANOVA on ranks, H=34.934, d.f.=8, $P\leq0.001$, N=13/24/11) (Fig. 5A).

Comparing the performance of the species on the same substrates in dry and wet conditions showed that the values of *S. inexpectata*

Journal of Experimental Biology (2023) 226, jeb244295. doi:10.1242/jeb.244295

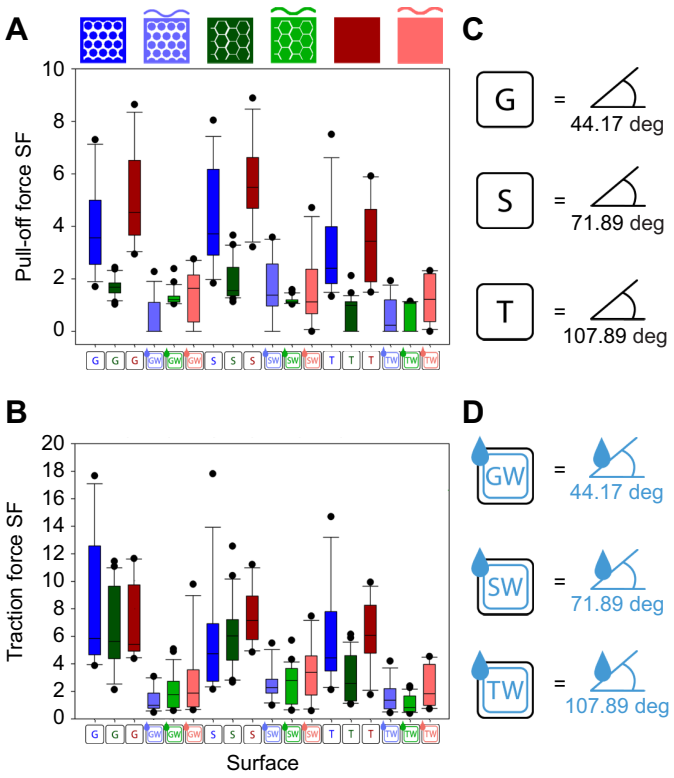

Fig. 5. Comparison of safety factors of the pull-off and traction forces between the three species on different surfaces. (A) Pull-off force safety factors and (B) traction force safety factors of *S. inexpectata* (blue; *n*=13), *E. nolimetangere* (green; *n*=24) and *M. extradentata* (red; *n*=11). The values correspond to the means of the triplet measurements per individual. Boxes indicate the 25th and 75th percentiles, whiskers are the 10th and 90th percentiles and the line within the boxes shows the median. Dark colors of the boxes indicate dry surfaces; light colors of the boxes indicate surfaces with a water film. (C,D) Pictograms indicating the different dry (C) and wet (D) surfaces (G, glass; S, silanized glass; T, Teflon; W, wet) with corresponding contact angles.

on G and T and those of *M. extradentata* on S were significantly different to those of their wet counterparts (Kruskal–Wallis one-way ANOVA on ranks, H=193.094, d.f.=17, $P \leq 0.001$, N=13/24/11).

Comparison of the traction force safety factors between the three species

All three species exhibited higher traction force safety factors on the dry surfaces than on the wet surfaces (*S. inexpectata*: G 8.57±4.88, S 5.59±4.15, T 5.83±3.67, GW 1.35±0.84, SW 2.57±1.20, TW 1.64±1.08; *E. nolimetangere*: G 6.65±3.01, S 6.17±2.52, T 2.92 ±1.74, GW 2.01±1.24, SW 2.64±1.38, TW 1.11±0.65; and *M. extradentata*: G 6.98±2.76, S 7.54±1.98, T 6.17±2.34, GW 2.74±2.79, SW 3.32±2.13, TW 2.40±1.40) (Fig. 5B), whereby only the values of *S. inexpectata* on G and T and the values of *E. nolimetangere* on G were significantly different to those for their wet counterpart (Kruskal–Wallis one-way ANOVA on ranks, H=172.383, d.f.=17, $P \leq 0.001$, N=13/24/11).

Comparing the dry surfaces, all values, except those of *S. inexpectata* on S and T, were significantly higher than the value for *E. nolimetangere* on T (Kruskal–Wallis one-way ANOVA on ranks, H=39.575, d.f.=8, $P \leq 0.001$, N=13/24/11).

For the wet surfaces, only the values of the three species on SW were significantly higher than the values of *E. nolimetangere* on TW (Kruskal–Wallis one-way ANOVA on ranks, H=32.172, d.f.=8, $P \leq 0.001$, N=13/24/11).

Loss of the pull-off force on wet surfaces compared with dry surfaces

The negative effect of water on the pull-off force was stronger for *M. extradentata* with smooth AMs and *S. inexpectata* with nubby AMs than for *E. nolimetangere* with hexagonal AMs on all substrates. *Medauroidea extradentata* exhibited a percentage loss in pull-of force of 73.07% on G versus GW, 69.83% on S versus SW and 40.04% on T versus TW, followed by *S. inexpectata* with 60.57% loss on G versus GW, 51.91% on S versus SW and 72.02% on T versus TW. The hexagonal AMs of *E. nolimetangere* showed a loss of attachment performance on G versus GW of 23.11%, on S versus SW of 31.90% and on T versus TW of 3.52% (Fig. 6A).

Loss of the traction force on wet surfaces compared with dry surfaces

The negative influence of water on the traction force on wet surfaces compared with dry surfaces was less pronounced than that for pull-off force among the three species. *Sungaya inexpectata* exhibited a percentage loss in traction force on G versus GW of 82.90%, on S versus SW of 46.75% and on T versus TW of 64.82%. *Epidares nolimetangere* showed a percentage loss in traction force on G versus GW of 63.52%, on S versus SW of 46.75% and on T versus TW of 45.80%. *Medauroidea extradentata* produced a percentage decrease of traction force on G versus GW of 57.44%, on S versus SW of 54.44% and on T versus TW of 24.12% (Fig. 6B).

Comparison of the pull-off force safety factors and the adhesive strength between all three species

As with the pull-off force safety factors, all species exhibited higher adhesive strength on dry surfaces than on wet surfaces (*M. extradentata*: G 10.72±4.94 kPa, GW 3.04±2.32 kPa, S 11.54±5.22 kPa, SW 2.42±1.42 kPa, T 7.13±4.23 kPa, TW 2.34±1,66 kPa; *S. inexpectata*: G 5.02±2.32 kPa, GW 0.48±0.76 kPa, S 5.45±2.88 kPa, SW 1.86±1.06 kPa, T 3.79±1.78 kPa, TW 0.81±0.88 kPa; and *E. nolimetangere*: G 3.10±0.67 kPa, GW 2.26±0.48 kPa, S 3.48±1.33 kPa, SW 2.17±0.44 kPa, T 1.14±1.12 kPa, TW 1.20±0.96 kPa).

In contrast to the mass-corrected data, the adhesion pad surface area-corrected data showed the following relationships. Between the dry surfaces, the values of *S. inexpectata* on G and S were not significantly different to the values of *E. nolimetangere* on G and S (Kruskal–Wallis one-way ANOVA on ranks, H=90.921, d.f.=8, $P \leq 0.001$, but Dunn's *post hoc* test P>0.05, N=13/24/11) (Fig. 7A). In contrast, the value of *E. nolimetangere* on G was significantly higher than the value of *E. nolimetangere* on T, and the value of *M. extradentata* on S was significantly higher than the value of *S. inexpectata* on T (Kruskal–Wallis one-way ANOVA on ranks, H=90.921, d.f.=8, $P \leq 0.001$, N=13/24/11).

When comparing the values on the wet surfaces, the performance of *S. inexpectata* on GW and TW differed noticeably between the mass-corrected and adhesion pad surface area-corrected data. For adhesive strength, only the values of *S. inexpectata* on SW and TW and of *E. nolimetangere* on TW were not significantly different to the value of *S. inexpectata* on GW. In addition, the values of *E. nolimetangere* on GW and SW and of *M. extradentata* on GW were significantly different to the values of *S. inexpectata* on TW, whereas the value of *S. inexpectata* on SW was no longer significantly different (Kruskal–Wallis one-way ANOVA on ranks, H=46.462, d.f.=8, $P \leq 0.001$, but Dunn's *post hoc* test P>0.05, N=13/24/11) (Fig. 7A).

Journal of Experimental Biology (2023) 226, jeb244295. doi:10.1242/jeb.244295

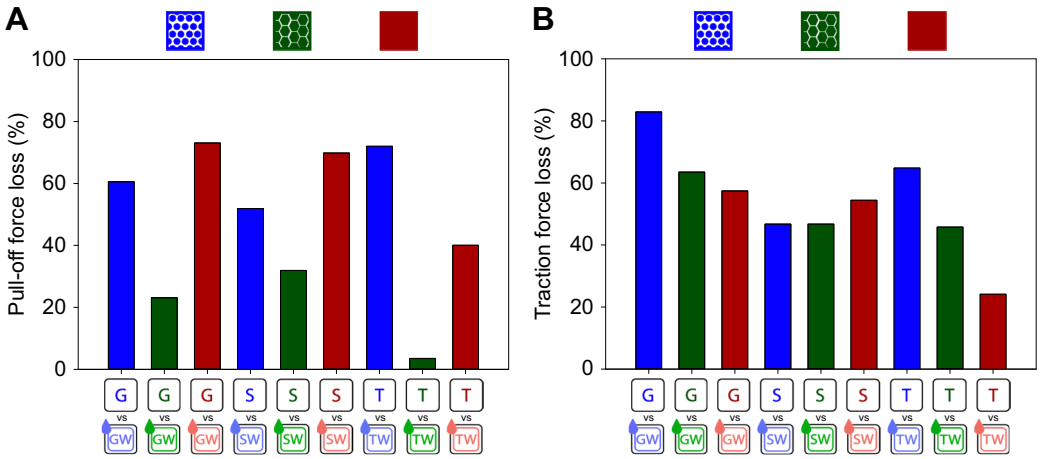

Fig. 6. Percentage of pull-off and traction force loss on wet surfaces compared with dry surfaces of the three species studied. (A) Percentage of pull-off force loss and (B) traction force loss on wet surfaces compared with dry surfaces for *S. inexpectata* (blue; *n*=13), *E. nolimetangere* (green; *n*=24) and *M. extradentata* (red; *n*=11). The pictograms represent the different dry and wet surfaces used (G, glass; S, silanized glass; T, Teflon; W, wet).

Comparison between the performance of the species on the same substrates in dry and wet conditions showed that only the value of *S. inexpectata* on S was significantly different (Kruskal–Wallis one-way ANOVA on ranks, H=193.051, d.f.=17, $P \leq 0.001$, N=13/24/11) (Fig. 7A).

Comparison of the traction force safety factor and the shear strength between all three species

As with the traction force safety factors, all species exhibited higher shear strength on dry surfaces than on wet surfaces (*M. extradentata*: G 14.22±6.17 kPa, GW 5.68±5.34 kPa, S 14.84±5.56 kPa, SW 5.70 ±2.76 kPa, T 12.14±5.68 kPa, TW 4.84±3.03 kPa; *S. inexpectata*: G 11.01±7.71 kPa, GW 1.56±0.84 kPa, S 7.17±4.92 kPa, SW 2.86±1.19 kPa, T 7.05±3.45 kPa, TW 2.19±1.33 kPa; and *E. nolimetangere*: G 11.93±4.55 kPa, GW 3.46±2.18 kPa, S 11.13±3.79 kPa, SW 5.05±2.76 kPa, T 5.05±2.80 kPa, TW 1.92 ±1.08 kPa) (Fig. 7B).

When comparing the performance on the dry surfaces, only a few differences were detected. The performance of *M. extradentata* on S was significantly different to the values of *S. inexpectata* on S and T. The performance of *S. inexpectata* on G was not significantly different to the value of *E. nolimetangere* on T (Kruskal–Wallis

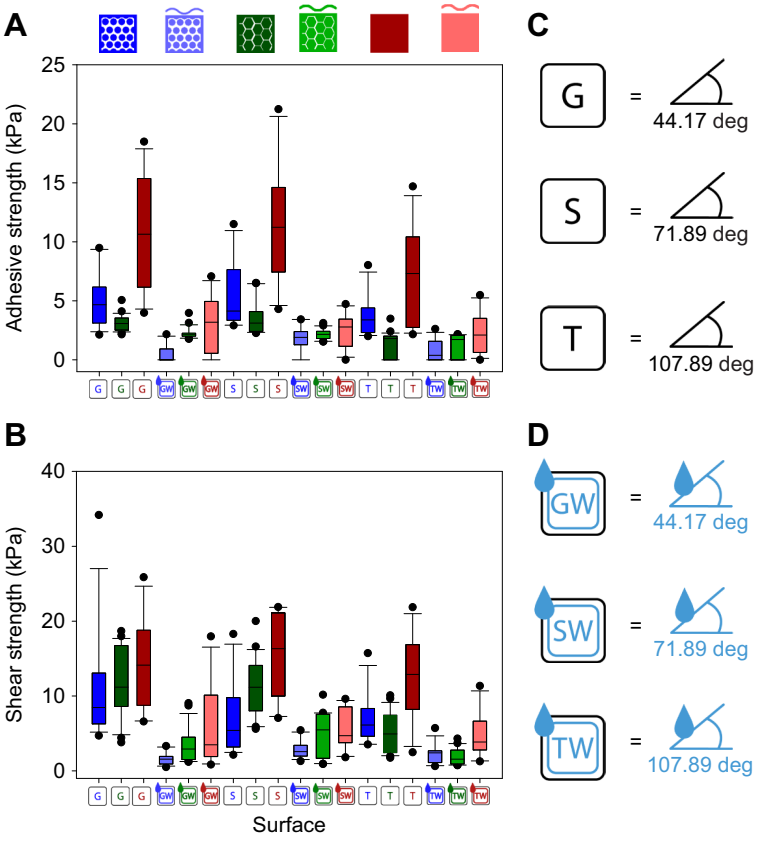

Fig. 7. Comparison of the adhesion and traction force divided by the surface area between all three species. (A) Adhesive strength and (B) shear strength of *S. inexpectata* (blue; *n*=13), *E. nolimetangere* (green; *n*=24) and *M. extradentata* (red; *n*=11). The values correspond to the means of the triplet measurements per individual. Boxes indicate the 25th and 75th percentiles, whiskers are the 10th and 90th percentiles and the line within the boxes shows the median. Dark colors of the boxes indicate dry surfaces; light colors of the boxes indicate surfaces with a water film. (C,D) Pictograms indicating the different dry (C) and wet (D) surfaces (G, glass; S, silanized glass; T, Teflon; W, wet) with corresponding contact angles.

one-way ANOVA on ranks, H=52.594, d.f.=8, P≤0.001, but Dunn's *post hoc* test P>0.05, N=13/24/11) (Fig. 7B).

On the wet surfaces, the performance of *S. inexpectata* on GW decreased, becoming significantly different from the values of *E. nolimetangere* on SW and *M. extradentata* on SW and TW. Other significant differences were measured between *M. extradentata* on SW and *S. inexpectata* on TW, and between *M. extradentata* on TW and *E. nolimetangere* on TW (Kruskal–Wallis one-way ANOVA on ranks, H=42.985, d.f.=8, P≤0.001, N=13/24/11) (Fig. 7B). No significant difference was measured between *S. inexpectata* on SW and *E. nolimentagere* on TW (Kruskal–Wallis one-way ANOVA on ranks, H=52.594, d.f.=8, P≤0.001, but Dunn's *post hoc* test P>0.05, N=13/24/11).

No significant difference was detected when comparing the performance of the species on the same substrates in dry and wet conditions (Kruskal–Wallis one-way ANOVA on ranks, H=177.160, d.f.=17, P≤0.001, N=13/24/11).

DISCUSSION

All three species were able to exert enough attachment force on all surfaces used in the experiments to hold more than their own weight (SF>1) (Fig. 5). Consequently, the tarsal attachment system of the three species can cope with the different SFE of the surfaces and the presence of water. Considering their habitats, this behavior was expected, as these insects are generally exposed to various natural substrate conditions (Heepe et al., 2017). Nevertheless, differences in the attachment performance were revealed among the three species, suggesting that the presence of water on the substrate and differences in the SFE of the substrate affect the three attachment systems to different extents.

Attachment performance on dry substrates

The attachment of animals using wet adhesion on dry substrates is mainly influenced by the interaction between the adhesive system, the adhesive secretion and the substrate surface.

The animals studied in these experiments possess smooth adhesive pads. This implies that the inner structure of the euplantulae and arolium consists of fibrils that are hierarchically organized, giving the attachment system certain flexibility (Perez-Goodwyn et al., 2006; Peisker et al., 2013; Bennemann et al., 2014), which allows the attachment devices to adapt to the surface profile up to a certain amplitude of roughness (Persson and Gorb, 2003; Eimüller et al., 2008; Gorb, 2011). As a result of this flexibility and the smooth surfaces used in our experiments (Teflon surface measured vertically: R_a=5.1±1.14 µm; Teflon surface measured horizontally: R_a=7.14±0.80 µm), the influence of the claws on attachment can be excluded (Büscher and Gorb, 2019).

One important factor that can influence the attachment performance of the species investigated in this study is the difference in their AMs. Because of the different AMs, the actual area of the adhesive contact, as well as the distribution of the adhesive fluid to the substrate, can differ greatly between the species studied here.

The actual adhesive contact area of *S. inexpectata* is reduced compared to the projected pad surface area as a result of the nubby AMs (Fig. 2C). Although the contact area increases by the deformation of the nubs under load, it remains smaller than that of a smooth-to-smooth contact (Labonte et al., 2014). The nubby AMs can distribute the adhesive fluid efficiently, which supports contact formation and strengthens the adhesion process (Arnold, 1974; Labonte and Federle, 2013; Büscher and Gorb, 2019; Büscher et al., 2020).

One advantage of the hexagonal AMs of *E. nolimetangere* is the formation of channels that can distribute the produced adhesive secretion evenly along the surface (Fig. 2G). Furthermore, the contact splitting reduces crack propagation as the pad is peeled off and avoids stick-and-slip motion of the pads (Johnson et al., 1971; Arzt et al., 2003; Meng et al., 2021). This has been shown for other insect species (Varenberg and Gorb, 2009) and tree frogs (Hanna and Barnes, 1990; Ba-Omar et al., 2000; Tsipenyuk and Varenberg, 2014; Meng et al., 2021).

Because of the smooth and unstructured AMs of *M. extradentata*, the actual adhesive area is not reduced (Fig. 2K). This also indicates that the secretion and distribution of the adhesive fluid cannot be supported by an additional structure (Büscher and Gorb, 2021).

Comparing the adhesive performance of the three species with a focus on the mass-corrected data (safety factor; Fig. 5) and adhesive pad surface area-corrected data (adhesive and shear strength; Fig. 7) shows that all species behave approximately the same. In this case, a comparison of the attachment performance between the three species using mass-corrected data is probably a better proxy than using projected adhesive pad surface area-corrected data, as the actual contact area of structured attachment pads is smaller than the measured projected area.

The second important factor influencing the attachment performance is the distribution and composition of the adhesive pad secretion. The presence of fluids in contacts implements capillary forces and viscous forces, increasing attachment strength (Langer et al., 2004; Ditsche and Summers, 2014). Additionally, the fluid fills nanoscale asperities of the substrate, increasing the actual contact area (Gorb et al., 2000). The secretions of phasmids and cockroaches consist of hydrophilic proteins and peptides as well as hydrophobic carbohydrates (Dirks and Federle, 2011; Betz et al., 2018), which together form a two-phasic secretion consisting of the hydrophilic and hydrophobic parts. However, the fluid may increase the distance between the two solid surfaces and thus reduce the contribution of van der Waals forces (Stefan, 1875; Kendall, 1994; Gorb, 2001; Varenberg and Gorb, 2008; Popov, 2016).

The insect cuticle as well as the adhesive secretion can be influenced by the SFE of the substrate. The hydrophobic cuticle of the adhesive pads could adhere better to a low SFE substrate, as stronger hydrophobic–hydrophobic interactions may occur (Bush et al., 2008; Gundersen et al., 2014). Furthermore, the SFE of the substrate could also influence the effect of the adhesive fluid on adhesive performance, as hydrophilic components of the secretion can interact better with surfaces with high SFE and hydrophobic components can interact better with surfaces with low SFE (Roth and Willis, 1952; Dixon et al., 1990; Büscher and Gorb, 2021).

An interesting result is the low pull-off force safety factor performance of *E. nolimetangere* on dry surfaces (Fig. 5A). This species possesses the smallest surface area of the arolium when compared with the other two species (*E. nolimetangere*: 0.13±0.02 mm^2; *M. extradentata*: 0.52±0.05 mm^2; *S. inexpectata*: 0.91±0.13 mm^2) (Fig. 2), which is most important for pull-off force generation (Labonte and Federle, 2013, 2015; Labonte et al., 2016), and thus provides the smallest potential adhesive area. Another result that stands out is the significant reduction of the pull-off force of *E. nolimetangere* on T (Fig. 5A), which could be explained by a reduction of the hydrophobic components of the pad secretion, in comparison to the other two species, whereby the secretion has a reduced influence on the attachment.

Medauroidea extradentata produces the highest pull-off force safety factors (Fig. 5A) as a consequence of the smooth unstructured AMs in combination with the medium-sized adhesive pad (*M. extradentata*: 5.30±0.82 mm^2; *E. nolimetangere*: 4.25±0.71 mm^2 and *S. inexpectata*: 20.74±3.20 mm^2). That smooth adhesive

structures show good adhesion to smooth surfaces has also been shown by other studies with Phasmatodea and other insect species (Drechsler and Federle, 2006; Bußhardt et al., 2012; Betz et al., 2017; Büscher et al., 2018a).

Similar effects of smooth substrates with different SFE on stick insect adhesion have been shown previously (Labonte et al., 2021). Their studied species *Carausius morosus* has nubby AMs similar to those of *S. inexpectata*. The substrates used there had water contact angles of 101, 16 and 5 deg. Labonte et al. (2021) showed that a decrease in contact angle correlates with a reduction in the attachment forces, but the attachment performance was still considerable. Our measurements with *S. inexpectata* showed a similar tendency (Fig. 5).

Experiments on the effect of SFE on the adhesion and traction of tree frogs that possess hexagonal AMs (*Osteopilus septentrionalis* and *Ranoidea caerulea*) showed that a decrease in SFE analogous to that used herein, i.e. from glass to silanized glass and further to Teflon, does not influence the generated forces significantly (Crawford, 2016). *Epidares nolimetangere*, the species with hexagonal AMs, displayed the same results on glass and silanized glass (Fig. 4C,D). However, the low SFE on Teflon resulted in significantly reduced pull-off forces and traction forces in this species of stick insect. This difference in attachment could be caused by the greater roughness of Teflon (Büscher and Gorb, 2019) and by a possible negative influence of the SFE on the adhesive secretion, potentially reducing its contribution to attachment.

Influence of surface water on the attachment performance

The significant reduction of the adhesion performance of all three types of AM on nearly all surfaces with a water film compared with the dry counterpart can be attributed to the negative effects of water on attachment (Figs 4–7).

In the case of flooded substrates, water has a negative influence on attachment forces (Labonte et al., 2021). Water tends to behave like a separating film between the two solid surfaces and increases the distance between them. Consequently, the van der Waals forces and the chemical bonds are significantly reduced (Hosoda and Gorb, 2012). Additionally, the capillary forces are reduced as a result of the surface tension approaching zero, as it is negatively affected by the thickness of the water film (Vogel, 2003; Gorb, 2001; Ditsche and Summers, 2014). In contrast, viscous forces are increased as a result of the higher viscosity of water compared with air (Stefan, 1875; Ditsche and Summers, 2014).

In addition to the physical forces, water could also influence the function of the adhesive secretion by dissolving its hydrophilic components and thus reducing their contribution to attachment. It is likely that the hydrophobic components of the adhesive secretion are not affected by the water, which indicates that their share in attachment is not influenced (Dirks and Federle, 2011; Betz et al., 2018; Büscher and Gorb, 2021).

To reduce the negative influence of water on attachment, the species try to displace it from the contact surface. Thus, a contact surface is created which is affected least by water. Different strategies have evolved that solve this problem, which are represented in this study by the different AMs (Fig. 2C,G,K) (Hosoda and Gorb, 2012; Büscher et al., 2018a; Büscher and Gorb, 2021).

The nubby AMs of *S. inexpectata* probably penetrate the water film to come into direct contact with the substrate (Arzt et al., 2003; Spolenak et al., 2005; Frost et al., 2018). In addition, it is likely that the water is directed into the hollow cavities created by the nubby structure to remove it from contact. This would further increase the real contact area and thus strengthen the attachment, explaining why the nubby AMs of *S. inexpectata* showed an intermediate effect on the percentage loss of attachment performance on wet surfaces (Fig. 6).

Previous research on hexagonal attachment structures has shown that they are most efficient in coping with water on surfaces (Barnes et al., 2006; Varenberg and Gorb, 2009; Drotlef et al., 2013; Endlein et al., 2013; Crawford, 2016; Meng et al., 2021; Tramsen et al., 2021). The channels on the pad surface can very effectively displace the water from the contact area, thus considerably increasing the real contact area. This is supported by our pull-off force experiments, as *E. nolimetangere* showed the lowest percentage loss of adhesion on the wet surfaces (Fig. 6A). However, the results with Teflon must be considered with caution, as the low adhesion already present on Teflon cannot be drastically affected by water (Figs 4C and 6A). What is noticeable, however, is that even on such an unfavorable surface, *E. nolimetangere* still produced enough adhesion to hold more than their own weight (Fig. 5A).

Medauroidea extradentata possesses smooth AMs and therefore would be expected to show the weakest performance on wet surfaces, as the flat, unstructured AMs cannot displace or penetrate the water film as effectively as those of the other two species. While the percentage loss of attachment indeed showed that *M. extradentata* produced the lowest attachment (Fig. 6A), it was observed that the attachment, once the pad had made contact, was still sufficient for the insects to hold more than their own weight (Fig. 5A).

The effects of substrate wetness on the attachment performance have also been studied in other insect species. Stark and Yanoviak (2018) showed that wetness influences the normal (pull-off) and shear (traction) adhesion of the smooth tarsal attachment system in the tropical arboreal ant *Cephalotes atratus*. Wetness reduced the normal and shear adhesion significantly on glass with a high SFE, but the normal adhesion on the surfaces with low SFE made of polycarbonate and polypropylene was unaffected (Stark and Yanoviak, 2018). *Medauroidea extradentata*, the stick insect with smooth AMs, showed the same results on glass, but the pull-off forces on the lower SFE silanized glass were significantly reduced (Fig. 4E). This discrepancy may be due to the fact that the two species represent different lineages of insects, which could have a different composition of the adhesive secretion and, consequently, different physico-chemical interactions between the pad material, secretion, water and substrate surface.

Labonte et al. (2021) have shown that both wetness and SFE influence the generated friction forces of *Carausius morosus*. The stick insect produced significantly reduced friction forces on wet smooth surfaces with high SFE compared with dry smooth surfaces with low SFE. Additionally, no significant difference was recorded when the wet and dry surfaces had a low SFE (Labonte et al., 2021). *Sungaya inexpectata*, which also possesses nubby AMs, like *C. morosus*, showed nearly the same results: both species displayed significantly reduced traction forces on wet surfaces with high SFE compared with those on dry surfaces with low SFE. However, while *C. morosus* showed similar traction forces on wet and dry surfaces with low SFE, *S. inexpectata* exerted significantly reduced friction forces on wet Teflon compared with dry Teflon (Fig. 4B). The difference between the two species may be due to differences in the composition and thickness of the adhesive secretion.

Differences between pull-off and traction forces

Differences in performance between the pull-off and traction force experiments in all three species were detected (Figs 4–6). During the

traction force experiments, the three species showed a more similar performance than during the pull-off force experiments. This could be explained by the fact that traction increases the effectiveness of water displacement from the contact surface regardless of the AM, because the application of traction forces mechanically removes water from the interface more efficiently (Peachey et al., 1991).

Conclusions

This study investigated and compared the effects of water films and surface chemistry on the attachment forces of three stick insect species with different AMs on their pads. We found the following: (1) the decrease in SFE does not significantly influence the pull-off forces and traction forces of the three stick insect species; (2) the presence of water reduces the pull-off and traction forces in all three species; and (3) all three species generate enough attachment force on all surfaces to adhere (SF>1). The AMs influence the effectiveness of attachment generation underwater. The AMs of *E. nolimetangere* had the strongest effect on attachment, the nubby AMs of *S. inexpectata* a medium effect and the smooth AMs of *M. extradentata* the least effect.

This study sheds light on how stick insects have adapted to varying environmental substrate conditions during their evolution. It shows how attachment pads with functional surface microstructures cope with such conditions. Nevertheless, many questions remain regarding the influence of the AMs and third bodies on the attachment performance, such as the ability to displace water, the generation of actual contact underwater, contamination and the effect of the adhesive secretion. Therefore, further investigations of such effects on attachment would be interesting. Furthermore, it would be intriguing to investigate how the actual distribution of the adhesive secretion on the AMs supports the function of each attachment system studied here.

Acknowledgements

We thank Esther Appel and Dr Alexander Kovalev (Department of Functional Morphology and Biomechanics, Kiel University Germany) for their technical assistance.

Competing interests

The authors declare no competing or financial interests.

Author contributions

Conceptualization: J.T., T.H.B.; Methodology: J.T., T.H.B.; Validation: J.T., T.H.B.; Formal analysis: J.T.; Investigation: J.T.; Resources: J.T., T.H.B.; Data curation: J.T., T.H.B.; Writing - original draft: J.T.; Writing - review & editing: S.G., T.H.B.; Visualization: J.T.; Supervision: T.H.B.; Project administration: S.G., T.H.B.; Funding acquisition: S.G.

Funding

This work was supported the Deutsche Forschungsgemeinschaft (grant GO 995/34-1) within the Special Priority Programme SPP 2100 'Soft Material Robotic Systems' to S.N.G.

Data availability

All relevant data can be found within the article and its supplementary information.

References

Arnold, J. W. (1974). Adaptive features on the tarsi of cockroaches (Insecta: Dictyoptera). *Int. J. Insect Morphol. Embryol.* **3**, 317-334. doi:10.1016/0020-7322(74)90026-9

Arzt, E., Gorb, S. N. N. and Spolenak, R. (2003). From micro to nano contacts in biological attachment devices. *Proc. Natl. Acad. Sci. USA* **100**, 10603-10606. doi:10.1073/pnas.1534701100

Attygall, A. B., Aneshansley, D. J., Meinwald, K. and Eisner, T. (2000). Defense by the foot adhesion in a chrysomelid beetle (*Hemisphaerota cyanea*): characterization of the adhesive oil. *Zoology* **103**, 1-6. doi:10.1073/pnas.97.12.6568

Bank, S., Cumming, R. T., Li, Y., Henze, K., Tirant, L. S. and Bradler, S. (2021a). A tree of leaves: phylogeny and historical biogeography of the leaf insects (Phasmatodea: Phylliidae). *Commun. Biol.* **4**, 932. doi:10.1038/s42003-021-02436-z

Bank, S., Buckley, T. R., Büscher, T. H., Bresseel, J., Constant, J., De Haan, M., Dittmar, D., Dräger, H., Kahar, R. S., Kang, A. et al. (2021b). Reconstructing the nonadaptive radiation of an ancient lineage of ground–dwelling stick insects (Phasmatodea: Heteropterygidae). *Sys. Entomol.* **46**, 487-507. doi:10.1111/syen.12472

Ba-Omar, T. A., Downie, J. R., Barnes, W. J. P. (2000). Development of adhesive toe-pads in the tree-frog (*Phyllomedusa trinitatis*). *J. Zool.* **250**, 267-282. doi:10.1111/j.1469-7998.2000.tb01077.x

Barnes, W. J. P., Oines, C. and Smith, J. M. J. (2006). Whole animal measurements of shear and adhesive forces in adult tree frogs: insights into underlying mechanisms of adhesion obtained from studying the effects of size and scale. *Comp. Physiol. A* **192**, 1179-1191. doi:10.1007/s00359-006-0146-1

Bedford, G. O. (1978). Biology and ecology of the Phasmatodea. *Ann. Rev. Entomol.* **23**, 125-149. doi:10.1146/annurev.en.23.010178.001013

Bennemann, M., Backhaus, S., Scholz, I., Park, D., Mayer, J. and Baumgartner, W. (2014). Determination of the Young's modulus of the epicuticle of the smooth adhesive organs of *Carausius morosus* using tensile testing. *J. Exp. Biol.* **217**, 3677-3687. doi:10.1242/jeb.105114

Betz, O., Frenzel, M., Steiner, M., Vogt, M., Kleemeier, M., Hartwig, A., Sampalla, B., Rupp, F., Boley, M. and Schmitt, C. (2017). Adhesion and friction of the smooth attachment system of the cockroach *Gromphadorhina portentosa* and the influence of the application of fluid adhesives. *Biol. Open* **6**, 589-601. doi:10.1242/bio.024620

Betz, O., Albert, K., Boley, M., Frenzel, M., Gerhard, H., Grunwald, I., Hartwig, A., Kleemeier, M., Maurer, A., Neunfeldt, M. et al. (2018). Struktur und Funktion des tarsalen Haftsystems der Madagaskar-Fauchschabe *Grompadorhina portentosa* (Blattodea). *Mitt. Dtsch. Ges. Allg. Angew. Ent.* **21**, 159-164.

Beutel, G. F. and Gorb, N. S. (2006). The attachment force on the dry substrates was considered as 100% attachment performance to calculate the remaining percentage of attachment on the corresponding wet surfaces. *Arthropod Syst. Phylogeny* **64**, 3-25.

Brock, P. D., Büscher, T. H. and Baker, E. (2022). Phasmida species file (Version 5.0). In *Species 2000 & ITIS Catalogue of Life* (ed. Y. Roskov, G. Ower, T. Orrell, D. Nicolson, N. Bailly, P. M. Kirk, T. Bourgoin, R. E. DeWalt, W. Decock, E. van Nieukerken and L. Penev) Species 2000. Leiden, The Netherlands: Naturalis. doi:10.48580/dfqj-398

Büscher, T. H. and Gorb, S. N. (2017). Subdivision of the neotropical Prisopodinae Brunner von Wattenwyl, 1893 based on features of tarsal attachment pads (Insecta, Phasmatodea). *ZooKeys* **645**, 1-11. doi:10.3897/zookeys.645.10783

Büscher, T. H. and Gorb, S. N. (2019). Complementary effect of attachment devices in stick insects (Phasmatodea). *J. Exp. Biol.* **222**, jeb209833. doi:10.1242/jeb.209833

Büscher, T. H. and Gorb, S. N. (2021). Physical constraints lead to parallel evolution of micro- and nanostructures of animal adhesive pads: a review. *Beilstein J. Nanotechnol.* **12**, 725-743. doi:10.3762/bjnano.12.57

Büscher, T. H., Buckley, T. R., Grohmann, C., Gorb, S. N. and Bradler, S. (2018a). The evolution of tarsal adhesive microstructures in stick and leaf insects (Phasmatodea). *Front. Ecol. Evol.* **6**, 69. doi:10.3389/fevo.2018.00069

Büscher, T. H., Kryuchkov, M., Katanaev, V. L. and Gorb, S. N. (2018b). Versatility of Turing patterns potentiates rapid evolution in tarsal attachment microstructures of stick and leaf insects (Phasmatodea). *J. R. Soc. Interface* **15**, 20180281. doi:10.1098/rsif.2018.0281

Büscher, T. H., Grohmann, C., Bradler, S. and Gorb, S. N. (2019). Tarsal attachment pads in Phasmatodea (Hexapoda: Insecta). *Zoologica* **164**, 1-94.

Büscher, T. H., Becker, M. and Gorb, S. (2020). Attachment performance of stick insects (Phasmatodea) on convex substrates. *J. Exp. Biol.* **223**, jeb226514. doi:10.1242/jeb.226514

Bush, J. W. M., Hu, D. L. and Prakash, M. (2008). The integument of water-walking arthropods: form and function. *Adv. Insect Phys.* **34**, 117-192. doi:10.1016/S0065-2806(07)34003-4

Bußhardt, P., Wolf, H. and Gorb, S. (2012). Adhesive and frictional properties of tarsal attachment pads in two species of stick insects (Phasmatodea) with smooth and nubby euplantulae. *Zoology* **115**, 135-141. doi:10.1016/j.zool.2011.11.002

Clemente, C. J. and Federle, W. (2008). Pushing versus pulling: division of labour between tarsal attachment pads in cockroaches. *Proc. R. Soc. B* **275**, 1329-1336. doi:10.1098/rspb.2007.1660

Crawford, N. A. (2016). The biomechanics of tree frog adhesion under challenging conditions. *PhD thesis*, University of Glasgow. http://theses.gla.ac.uk/7102/

Cumming, R. T., Le Tirant, S. and Büscher, T. H. (2021). Resolving a century-old case of generic mistaken identity: polyphyly of *Chitoniscus* sensu lato resolved with the description of the endemic New Caledonia *Trolicaphyllium* gen. nov. (Phasmatodea, Phylliidae). *ZooKeys* **1055**, 1-41. doi:10.3897/zookeys.1055.66796

Dirks, J. H. (2014). Physical principles of fluid-mediated insect attachment - shouldn't insects slip? *Beilstein J. Nanotechnol.* **5**, 1160-1166. doi:10.3762/bjnano.5.127

Dirks, J. H. and Federle, W. (2011). Fluid-based adhesion in insects – principles and challenges. *Soft Mat.* **7**, 11047-11053. doi:10.1039/c1sm06269g

Dirks, J. H., Clemente, C. J. and Federle, W. (2010). Insect tricks: two-phasic foot pad secretion prevents slipping. *J. R. Soc. Interface* **7**, 587-593. doi:10.1098/rsif.2009.0308
Ditsche, P. and Summers, A. P. (2014). Aquatic versus terrestrial attachment: water makes a difference. *Beilstein J. Nanotechnol.* **5**, 2424-2439. doi:10.3762/bjnano.5.252
Dixon, A. F. G., Croghan, P. C. and Gowing, R. P. P. (1990). The mechanism by which aphids adhere to smooth surfaces. *J. Exp. Biol.* **152**, 243-253. doi:10.1242/jeb.152.1.243
Drechsler, P. and Federle, W. (2006). Biomechanics of smooth adhesive pads in insects: influence of tarsal secretion on attachment performance. *J. Comp. Physiol. A.* **192**, 1213-1222. doi:10.1007/s00359-006-0150-5
Drotlef, D. M., Stepien, L., Kappl, M., Barnes, W. J. P., Butt, H. J. and Del Campo, A. (2013). Insights into the adhesive mechanisms of tree frogs using artificial mimics. *Adv. Funct. Mater.* **23**, 1137-1146. doi:10.1002/adfm.201202024
EimüLler, T., Guttmann, P. and Gorb, S. N. (2008). Terminal contact elements of insect attachment devices studied by transmission X-ray microscopy. *J. Exp. Biol.* **211**, 1958-1963. doi:10.1242/jeb.014308
Endlein, T., Barnes, W. J. P., Samuel, D. S., Crawford, N. A., Biaw, A. B. and Grafe, U. (2013). Sticking under wet conditions: the remarkable attachment abilities of the torrent frog, *Staurois guttatus*. *PLoS One* **8**, e73810. doi:10.1371/journal.pone.0073810
England, M. W., Sato, T., Yagihashi, M., Hozumi, A., Gorb, S. N. and Gorb, E. V. (2016). Surface roughness rather than surface chemistry essentially affects insect adhesion. *Beilstein J. Nanotechnol.* **7**, 1471-1479. doi:10.3762/bjnano.7.139
Federle, W. (2006). Why are so many adhesive pads hairy? *J. Exp. Biol.* **209**, 2611-2621. doi:10.1242/jeb.02323
Federle, W., Rohrseitz, K. and Hölldobler, B. (2000). Attachment forces of ants measured with a centrifuge: better "wax-runners" have a poorer attachment to a smooth surface. *J. Exp. Biol.* **203**, 505-512. doi:10.1242/jeb.203.3.505
Federle, W., Barnes, W. J. P., Baumgartner, W., Drechsler, P. and Smith, J. M. (2006). Wet but not slippery: boundary friction in tree frog adhesive toe pads. *J. R. Soc. Interface* **3**, 689-697. doi:10.1098/rsif.2006.0135
Frost, K. F., Gorb, S. N. and Wolff, J. O. (2018). Adhesion and friction in hunting spiders: the effect of contact splitting on their attachment ability. *Zool. Anz.* **273**, 231-239. doi:10.1016/j.jcz.2018.01.003
Gorb, S. N. (2001). *Attachment Devices of Insect Cuticle*. Dordrecht: Springer.
Gorb, S. N. (2011). Biological fibrillar adhesives: functional principles and biomimetic applications. In *Handbook of Adhesion Technology* (ed. L. F. M. da Silva, A. Öchsner and R. D. Adams), pp. 1409-1436. Berlin: Springer.
Gorb, E. V. and Gorb, S. N. (2009). Effects of surface topography and chemistry of *Rumex obtusifolius* leaves on the attachment of the beetle *Gastrophysa viridula*. *Entomol. Exp. Appl.,* **130**, 222-228. doi:10.1111/j.1570-7458.2008.00806.x
Gorb, E. V. and Gorb, S. N. (2017). Anti-adhesive effects of plant wax coverage on insect attachment. *J. Exp. Bot.,* **68**, 5323-5337. doi:10.1093/jxb/erx271
Gorb, S. N., Jiao, Y. and Scherge, M. (2000). Ultrastructural architecture and mechanical properties of attachment pads in *Tettigonia viridissima* (Orthoptera Tettigoniidae). *J. Comp. Physiol. A* **186**, 821-831. doi:10.1007/s003590000135
Gottardo, M. and Vallotto, D. (2014). External macro-and micromorphology of the male of the stick insect *Hermarchus leytensis* (Insecta: Phasmatodea) with phylogenetic considerations. *C. R. Biol.* **337**, 258-268. doi:10.1016/j.crvi.2014.02.005
Gundersen, H., Leinaas, H. P. and Thaulow, C. (2014). Surface structure and wetting characteristics of *Collembola* cuticles. *PLoS One* **9**, e86783. doi:10.1371/journal.pone.0086783
Hanna, G. and Barnes, W. J. P. (1990). Adhesion and detachment of the toe pads of tree frogs. *J. Exp. Biol.* **155**, 103-125. doi:10.1242/jeb.155.1.103
Heepe, L., Xue, L. and Gorb, S. N. (2017). *Bio-Inspired Structured Adhesives*. Cham: Springer.
Hosoda, N. and Gorb, S. N. (2012). Underwater locomotion in a terrestrial beetle: combination of surface de-wetting and capillary forces. *Proc. R. Soc. Lond. B* **279**, 4236-4242. doi:10.1098/rspb.2012.1297
Jiao, Y., Gorb, S. N. and Scherge, M. (2000). Adhesion measured on the attachment pads of *Tettigonia viridissima* (Orthoptera, Insecta). *J. Exp. Biol.* **203**, 1887-1895. doi:10.1242/jeb.203.12.1887
Johnson, K. L. (1998). Mechanics of adhesion. *Tribol. Int.* **31**, 413-418. doi:10.1016/S0301-679X(98)00060-7
Johnson, K. L., Kendall, K. and Roberts, A. D. (1971). Surface energy and the contact of elastic solids. *Proc. R. Soc. Lond. A* **324**, 301-313. doi:10.1098/rspa.1971.0141
Kendall, K. (1994). Adhesion: molecules and mechanics. *Science* **263**, 1720-1725. doi:10.1126/science.263.5154.1720
Labonte, D. and Federle, W. (2013). Functionally different pads on the same foot allow control of attachment: stick insects have load-sensitive ''Heel'' pads for friction and shear-sensitive ''Toe'' pads for adhesion. *PLoS One* **8**, e81943. doi:10.1371/journal.pone.0081943
Labonte, D. and Federle, W. (2015). Scaling and biomechanics of surface attachment in climbing animals. *Philos. Trans. R. Soc. B* **370**, 20140027. doi:10.1098/rstb.2014.0027
Labonte, D., Williams, A. and Federle, W. (2014). Surface contact and design of fibrillar 'friction pads' in stick insects (*Carausius morosus*): mechanisms for large friction coefficients and negligible adhesion. *J. R. Soc. Interface* **11**, 20140034. doi:10.1098/rsif.2014.0034
Labonte, D., Clemente, C. J., Dittrich, A., Kuo, C.-Y., Crosby, A. J., Irschick, D. J. and Federle, W. (2016). Extreme positive allometry of animal adhesive pads and the size limits of adhesion-based climbing. *Proc. Natl. Acad. Sci. USA* **113**, 1297-1302. doi:10.1073/pnas.1519459113
Labonte, D., Robinson, A., Bauer, U. and Federle, W. (2021). Disentangling the role of surface topography and intrinsic wettability in the prey capture mechanism of *Nepenthes* pitcher plants. *Acta Biomater.* **119**, 225-233. doi:10.1016/j.actbio.2020.11.005
Langer, M. G., Ruppersberg, J. P. and Gorb, S. N. (2004). Adhesion forces measured at the level of a terminal plate of the fly's seta. *Proc. R. Soc. B* **271**, 2209-2215. doi:10.1098/rspb.2004.2850
Meng, L., Shi, L. and Wang, X. (2021). Physical mechanisms behind the wet adhesion: from amphibian toe-pad to biomimetics. *Colloids Surf. B* **199**, 111531. doi:10.1016/j.colsurfb.2020.111531
Peachey, J., Van Alsten, J. and Granick, S. (1991). Design of an apparatus to measure the shear response of ultrathin liquid films. *Rev. Sci. Instrum.* **62**, 463-473. doi:10.1063/1.1142089
Peisker, H., Michels, J. and Gorb, S. N. (2013). Evidence for a material gradient in the adhesive tarsal setae of the ladybird beetle *Coccinella septempunctata*. *Nat. Commun.* **4**, 1661. doi:10.1038/ncomms2576
Perez-Goodwyn, P., Peressadko, A., Schwarz, H., Kastner, V. and Gorb, S. N. (2006). Material structure, stiffness, and adhesion: why attachment pads of the grasshopper (*Tettigonia viridissima*) adhere more strongly than those of the locust (*Locusta migratoria*) (Insecta: Orthoptera*). J. Comp. Physiol. A* **192**, 1233-1243. doi:10.1007/s00359-006-0156-z
Persson, B. N. J. (2003). On the mechanism of adhesion in biological systems. *J. Chem. Phys.* **118**, 7614. doi:10.1063/1.1562192
Persson, B. N. J. and Gorb, S. N. (2003). The effect of surface roughness on the adhesion of elastic plates with application to biological systems. *J. Chem. Phys.* **119**, 11437. doi:10.1063/1.1621854
Pohl, H. (2010). A scanning electron microscopy specimen holder for viewing different angles of a single specimen. *Microsc. Res. Tech.* **73**, 1073-1076.
Popov, V. L. (2016). *Kontaktmechanik und Reibung: Von der Nanotribologie bis zur Erdbebendynamik*. Berlin Heidelberg: Springer.
Roth, L. M. and Willis, E. R. (1952). A study of cockroach behavior. *Am. Midl. Nat.* **47**, 66-129. doi:10.2307/2421700
Scherge, M. and Gorb, S. N. (2001). *Biological Micro- and Nanotribology*. Berlin Heidelberg: Springer.
Spolenak, R., Gorb, S. N., Gao, H. and Arzt, E. (2005). Effects of contact shape on the scaling of biological attachments. *Proc. R. Soc. A* **461**, 305-319. doi:10.1098/rspa.2004.1326
Stark, A. Y. and Yanoviak, S. P. (2018). Adhesion and running speed of a tropical arboreal ant (*Cephalotes atratus*) on wet substrates. *R. Soc. Open Sci.* **5**, 181540. doi:10.1098/rsos.181540
Stefan, J. (1875). Versuche zur scheinbaren Adhesion. In *Annalen der Physik und Chemie*, vol. 154 (ed. J. J. Poggenorf), pp. 316-318. Leipzig, Germany: Verlag von Johan Ambrosius Barth.
Tramsen, H. T., Heepe, L. and Gorb, S. N. (2021). Granular media friction pad for robot shoes – hexagon patterning enhances friction on wet surfaces. *Appl. Sci.* **11**, 11287. doi:10.3390/app112311287
Tsipenyuk, A. and Varenberg, M. (2014). Use of biomimetic hexagonal surface texture in friction against lubricated skin. *J. R. Soc. Interface* **11**, 20140113. doi:10.1098/rsif.2014.0113
Varenberg, M. and Gorb, S. N. (2008). A beetle-inspired solution for underwater adhesion. *J. R. Soc. Interface* **5**, 383-385. doi:10.1098/rsif.2007.1171
Varenberg, M. and Gorb, S. N. (2009). Hexagonal surface micropattern for dry and wet friction. *Adv. Mater.* **21**, 483-486. doi:10.1002/adma.200802734
Vötsch, W., Nicholson, G., Müller, R., Stierhof, D. Y., Gorb, N. S. and Schwarz, U. (2002). Chemical composition of the attachment pad secretion of the locust Locusta migratoria. *Insect Biochem. Mol. Biol.* **32**, 1605-1613. doi:10.1016/S0965-1748(02)00098-X
Vogel, S. (2003). *Comparative Biomechanics - Life's Physical Word*. Princeton University Press.
Voigt, D. and Gorb, S. N. (2009). Egg attachment of the asparagus beetle Crioceris asparagi to the crystalline waxy surface of Asparagus officinalis. *Proc. R. Soc. B Biol. Sci.* **277**, 895-903. doi:10.1098/rspb.2009.1706
Wang, M., Béthoux, O., Bradler, S., Jacques, F. M. B., Cui, Y. and Ren, D. (2014). Under cover at pre-angiosperm times: a cloaked phasmatodean insect from the early cretaceous Jehol biota. *PLoS One* **9**, e91290. doi:10.1371/journal.pone.0091290